

# Learning to Terminate in Object Navigation

**Yuhang Song** \*

*Department of Computer Science  
University of Liverpool*

SGYSON10@LIVERPOOL.AC.UK

**Anh Nguyen**

*Department of Computer Science  
University of Liverpool*

ANH.NGUYEN@LIVERPOOL.AC.UK

**Chun-Yi Lee**

*Department of Computer Science  
National Tsing Hua University*

CYLEE@CS.NTHU.EDU.TW

**Editors:** Berrin Yanıkoğlu and Wray Buntine

## Abstract

This paper tackles the critical challenge of object navigation in autonomous navigation systems, particularly focusing on the problem of target approach and episode termination in environments with long optimal episode length in Deep Reinforcement Learning (DRL) based methods. While effective in environment exploration and object localization, conventional DRL methods often struggle with optimal path planning and termination recognition due to a lack of depth information. To overcome these limitations, we propose a novel approach, namely the Depth-Inference Termination Agent (DITA), which incorporates a supervised model called the Judge Model to implicitly infer object-wise depth and decide termination jointly with reinforcement learning. We train our judge model along with reinforcement learning in parallel and supervise the former efficiently by reward signal. Our evaluation shows the method is demonstrating superior performance, we achieve a 9.3% gain on success rate than our baseline method across all room types and gain 51.2% improvements on long episodes environment while maintaining slightly better Success Weighted by Path Length (SPL). Code and resources, visualization are available at: [https://github.com/HuskyKingdom/DITA\\_acml2023](https://github.com/HuskyKingdom/DITA_acml2023)

**Keywords:** Visual navigation, Supervised learning, Deep Reinforcement learning

## 1. Introduction

Object navigation represents a critical challenge within the realm of autonomous navigation (Bagnell et al., 2010), it necessitates the ability of robotic agents to navigate proficiently within environments that have not been previously encountered. The primary goal is to reach a specified target object, and the successful completion of this task is contingent upon the agent’s ability to self-declare the successful attainment of the target object, thereby concluding the episode. Such tasks may seem straightforward from a human perspective given our inherent knowledge and comprehension of the essential conditions required for successful navigation (Wang et al., 2022). Humans, for example, possess an intuitive sense

---

\* The author is affiliated with the Department of Computer Science, National Tsing Hua University as well in a dual Ph.D. program.

of where to begin exploring, as certain objects have a higher likelihood of being found in specific areas. Moreover, upon visually spotting the desired object, we instinctively plan an optimal route toward the target. Drawing inspiration from human problem-solving strategies, we could break down the task into two phases: (i) Explore the environment and locate the target object. (ii) Navigate to the target object until it is reached, then declare episode termination.

The underlying principle of Deep Reinforcement Learning methods (DRL) of maximizing the cumulative reward, inherently aligned with the goal of effective exploration and object localization, led to their extensive use within the field. [Mirowski et al. \(2016\)](#); [Zhu et al. \(2017\)](#) trained agents to perform navigation behaviors by encoding visual observation of the agent with its relevant states as embedding and passing that to A3C ([Mnih et al., 2016](#)) Reinforcement Learning model with the recurrent neural network. [Wortsman et al. \(2019\)](#) adopts a meta-learning approach with reinforcement learning, where it learns a self-supervised interaction loss during the inference process, to help prevent collisions. Moreover, By considering semantic context, just like how pre-knowledge of human beings take part, [Yang et al. \(2018\)](#); [Pal et al. \(2021\)](#); [Druon et al. \(2020\)](#); [Du et al. \(2020\)](#) propose to incorporate scene prior of the object relations with Graph Neural Network (GCN) embedded to the network for the agent to better explores the environment. Despite the promising outcomes demonstrated by Deep Reinforcement Learning (DRL) based methods in exploration and object localization, their application in environments characterized by extended optimal episode lengths presents distinct challenges. They often struggle to address optimal path planning to the object and termination recolonization ([Kartal et al., 2019](#)). In these scenarios, our observations indicate that after the agent has seen the target object, it often still fails to keep approaching the target. These limitations become even more pronounced in object navigation, where the agents are expected to declare the termination of the episode on its own in unseen environments with the absence of depth information. Given that objects of varying types often exhibit different sizes, it becomes challenging for DRL agents to discern the dependencies between their actions and the task at hand without explicit depth information pertaining to the object, resulting in the navigation agent falling into local maximums ([Jaakkola et al., 1994](#)), in which it avoids step penalty by terminating the episode in the early stage in environments ([Ren et al., 2022](#)).

Building on these insights, we introduce an innovative approach to object navigation that harnesses the power of Deep Reinforcement Learning (DRL) rewards to guide a model in inferring depth implicitly. Our method introduces a model called the *Judge Model*, a supervised classification model trained in conjunction with the DRL agent and guided by the DRL reward signal. The Judge Model’s role is to assess the appropriate termination time for the DRL agent by implicitly estimating object depth based on the results of object detection. We integrate our judge model as part of the agent, enabling the DRL agent to explore the unseen environment while searching for the target. Once the target appears in the observation frame, the judge model provides a termination confidence level. The agent then decides whether to terminate the episode based on the outputs from both models as shown in [Figure 1](#). We evaluate our proposed DITA model in AI2-THOR framework ([Kolve et al., 2017](#)), a platform that furnishes highly customizable environments, and permits the agent to enact navigation actions within these environments, subsequently observing the changes induced by those actions.

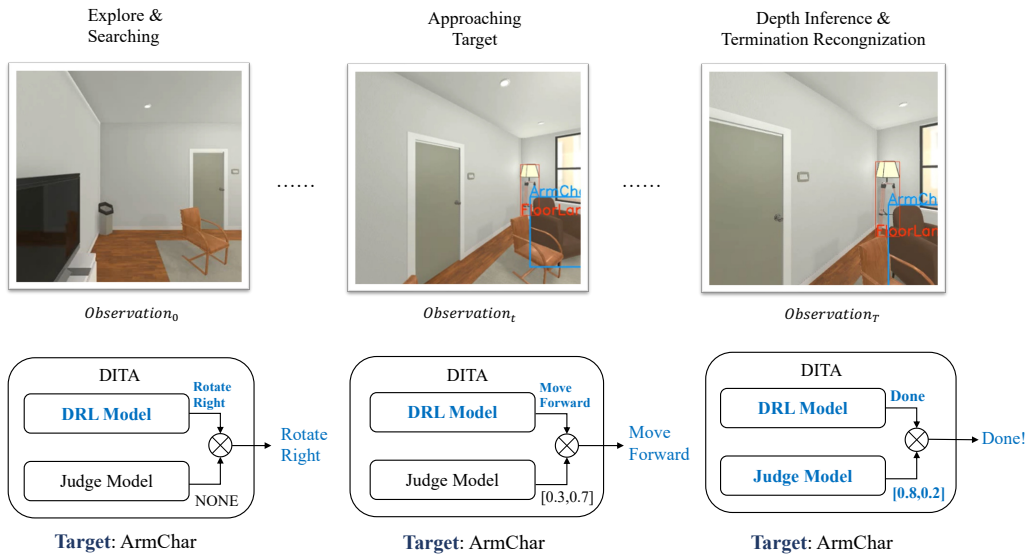


Figure 1: Depth-Inference Termination Agent (DITA) Model Overview. Upon sense observation from time step  $t$ , the DRL model embeds the observation into  $StateEmb_t$ , this embedding is then sent to the judge model to classify whether to sample termination action, based on both output from DRL and the judge model, our DITA model outputs the final action  $a_t$ .

Our contributions are summarized as follows: (1) We build a supervised model called judge model to recognize termination by implicitly inference object depth. (2) The integration of the judge model with a backbone DRL, training them simultaneously. (3) Our experiment result demonstrates the generalizability of implicit depth inference to unseen environments, DITA outperforms previous pure reinforcement learning-based methods.

The remaining of the paper is organized as the following, section 2 introduces related works in the field, then we demonstrate our main approach and discuss the definition of object navigation task in 3. In section 4 we will go through the dataset we used, with experiment designs and results, then end by section 5 where we will summarize our work and discuss possible future works.

## 2. Related Work

**Map-based Navigation.** Visual Navigation refers to the tasks that with visual input for an agent to navigate. Traditional methodologies primarily focused on solving navigation problems by building explicit models of the environment in the agent’s memory through interaction, enabling inference from the obtained knowledge (Oriolo et al., 1995; Milani et al., 2023; Chaplot et al., 2020a,b; Ramakrishnan et al., 2022). This knowledge usually consists of environmental maps and additional prior knowledge. With the advent of Simultaneous Localization and Mapping (SLAM) (Fuentes-Pacheco et al., 2015), a modular and hierarchical approach was proposed to construct explicit environment maps for both exploration and inference (Chaplot et al., 2020a). Subsequent studies include Chaplot et al.

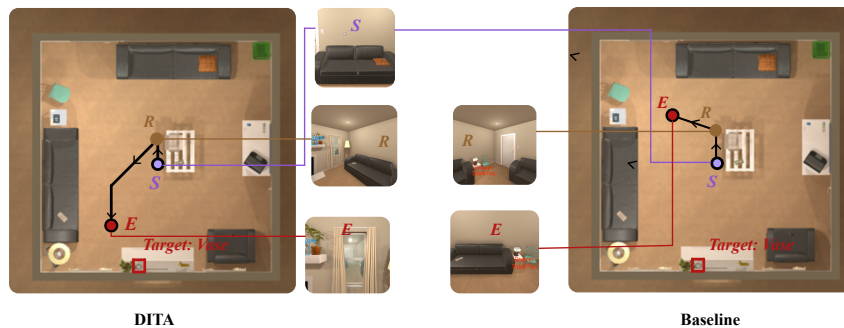


Figure 2: Trajectories of DITA and MJOLNIR-o baseline in FloorPlan 225. Point  $S$  is where the agent is initialized,  $E$  is where the agent samples termination action,  $R$  is where the agent rotates around to find the target. The baseline model rotates and ends the episode before it finds the target, whereas our DITA agent does not end the episode until it is confident enough.

(2020b) integrated semantic priors into the environment model, resulting in maps with semantic priors. Inferences were made on learned semantic knowledge, and a pre-trained potential function network was used to predict target potential areas from the generated top-down semantic maps (Ramakrishnan et al., 2022). Our work deviates from these conventional approaches as our navigation model is not based on any maps, our model learns the exploration policy and target recognition simultaneously. Recently, a proposal to maintain a topological map-like Hierarchical Object-to-Zoo (HOZ) graph during navigation was made (Zhang et al., 2021), allowing agents to perform optimal path planning. However, the HOZ graph requires significant manual design and configuration, limiting its flexibility and adaptability in varied or unpredictable environments. Our approach differs by learning more generalizable implicit depth information.

**Map-less Navigation.** Due to the computational complexity and memory consumption of map-based methods, especially when constructing maps in complex environments, more attention has been directed towards map-less deep reinforcement learning models (Khandelwal et al., 2022; Zhu et al., 2021; Dinh Vuong et al., 2023; Ye et al., 2021; Fukushima et al., 2022). These models usually encode the current states of the agent into an embedding and feed it into deep reinforcement learning models. These can be broadly classified into those that use more informative encoders or those based on Recurrent Neural Networks (RNN) (Mirowski et al., 2016; Zhu et al., 2017; Savva et al., 2017; Yang et al., 2018; Pal et al., 2021; Ramrakhya et al., 2022; Wijmans et al., 2023). Our work belongs to this latter category, but unlike the others, we consider estimating depth on an object-wise basis. Additionally, an alternative approach in the literature combines imitation learning with reinforcement learning frameworks (Du et al., 2020, 2021). While the fusion of imitation and reinforcement learning presents an interesting approach, our work aims to maximize the efficiency and effectiveness of a combination of reinforcement learning and self-supervised signals. Our approach is applicable to both exploration and exploitation, even in the absence of suitable expert demonstrations.

**Problem of Local Maxima.** The issue of local maxima is a significant challenge in Reinforcement Learning. This problem, which arises from sparse rewards, hinders agents from achieving the optimal solution in complex environments with extensive action spaces. Current solutions to these problems include either leveraging existing data of the agent itself, for example, encouraging the agent to explore more on new states (Ostrovski et al., 2017; Pathak et al., 2017; Stadie et al., 2015; Haarnoja et al., 2018), or learning from states with no reward (Andrychowicz et al., 2017). Alternatively by making use of external guidance, either through Reward Shaping (Hu et al., 2020; Devlin and Kudenko, 2012), Imitation Learning (Ho and Ermon, 2016; Ramrakhya et al., 2022) or Curriculum Learning (Soviany et al., 2022). However, these methods essentially presuppose the agent’s incapacity to terminate the episode independently, which aids the exploration of diverse state possibilities in complex environments. In our context, the diverse representations of different room types and the agent’s capability to enact termination action make these traditional methods less applicable or insufficiently effective. Additionally, existing exploration encouragement methods such as curiosity-driven exploration (Pathak et al., 2017) might need to be adapted to ensure the agent explores not only the states but also the potential termination points effectively. Instead, we directly train a judge model alongside Reinforcement Learning to only allow the agent to actively terminate when it is confident enough.

**Depth Inference.** Depth Inference refers to the prediction of depth maps using RGB images. This area is well-established within the field of Computer Vision, as demonstrated by a plethora of studies (Laina et al., 2016; Zhou et al., 2017; Zheng et al., 2018; Ranjan et al., 2019). Nonetheless, directly translating these depth estimation methodologies into our context introduces several complications. These models were initially designed either to estimate precise depth maps over the whole frame or require labeled training data in certain scenarios, direct application of these depth estimation methods into our scenarios can lead to high computational overhead or inefficiency. Conversely, our proposed method capitalizes on the results of object detection. By directly learning from the reward signal of the environment, our model implicitly infers depth information solely on specific objects of interest to determine whether to terminate the episode, making it more suitable for the task.

### 3. Learning to Terminate in Object Navigation

#### 3.1. Definition of Object Navigation

Consider an environment set that has object types  $C = \{c_1, c_2, \dots, c_n\}$ , the aim of object navigation is to navigate to a specified object type  $c_{target} \in C$ , e.g., an "ArmChair" or "Pillow". The agent is initially placed randomly in state  $t_0$ . At each time step  $t$ , it takes observation  $o_t$  and acts in the environment.  $o_t \in O$  is a visual input of RGB image captured by the agent’s camera, whereas the agent has the action space of six discrete actions  $a_t \in A = \{MoveAhead, RotateLeft, RotateRight, LookUp, LookDown, Done\}$ . The action *MoveAhead* propels the agent forward 0.25m, rotational actions turn the agent 45° to the left or right, and look actions adjust the camera by 30° upwards or downwards. The action *Done* enables the agent to declare success and terminate the episode. Episode termination can occur due to various conditions, including the agent’s active decision to terminate or when the episode reaches its maximum predefined length. An episode is deemed successful

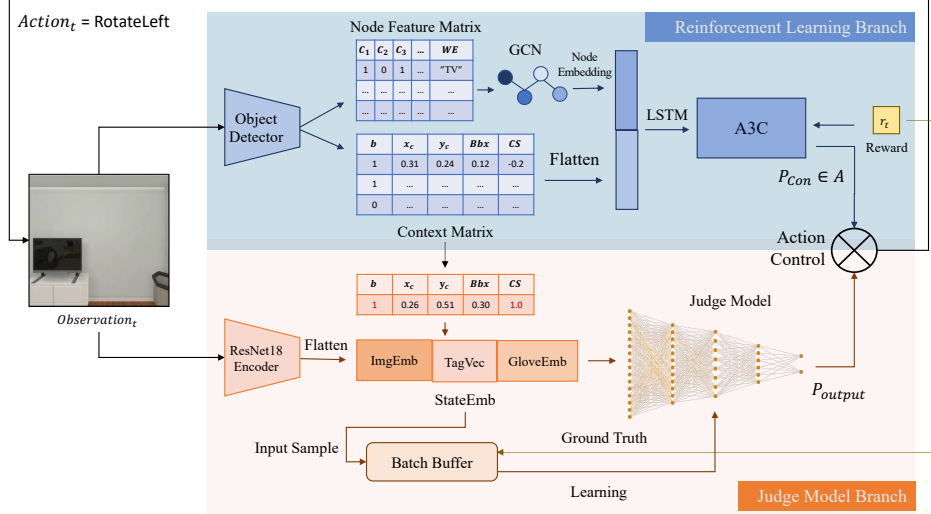


Figure 3: DITA Architecture.  $Observation_t$  is passed into both the reinforcement learning branch and judge model branch, where the reinforcement learning branch outputs *control action distributions*  $P_{con}$ , and judge model outputs termination action distribution defined as  $P_{output} = [p_d, p_n]$ , action control receives these two distributions and decides the final output action  $a_t$

if the agent actively terminates with the target object within the observation frame and the distance between the agent and the target object is less than 1.5m.

### 3.2. Method

**Deep Reinforcement Learning Branch.** Given the impressive capabilities of enriched environment exploration ability of MJOLNIR-o (Pal et al., 2021), we use it as our backbone reinforcement learning model. Upon receiving the observation, the model builds a 2D array in shape  $(N_C, N_C + 300)$  called Node Feature Matrix by processing the result from a ground-truth object detector, where  $N_C = |C|$  is the number of object types across all rooms. Each row of the Node Feature Matrix would be passed as an individual input node feature pass to the corresponding GCN node, with its first  $N_C$  columns standing for a binary vector indicating the object detection result for all object types  $C$ , and the last 300 elements is a GloVe word embedding (Pennington et al., 2014) vector of the current object. Node embedding is learned through a graph neural network that was made by object relation labels provided by Visual Genome (VG) dataset (Krishna et al., 2017) and pruned some relations off for AI2-THOR objects. On the other hand, the model also constructs Context Matrix from object detection, with each row representing a vector containing the object detection state of an object type  $c \in C$  with  $row_c = \{b, x_c, y_c, Bbx, CS\}$ ,  $b$  is a binary indicator represents whether an object with type  $c$  is visible in the current frame,  $x_c$  and  $y_c$  is the coordinates of object detection bounding box center,  $Bbx$  is the bounding box area, and the  $CS$  is the cosine similarity of word embedding vectors between object type  $c$  and the target object type, defined as:  $CS(G_c, G_{target}) = \frac{G_c \cdot G_{target}}{\|G_c\| \cdot \|G_{target}\|}$ .  $G_c$  and  $G_{target}$  are GloVe vectors for the current object and target object respectively.

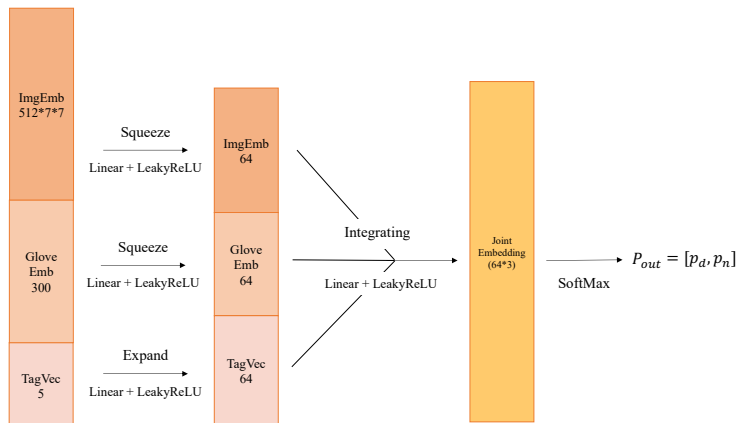


Figure 4: Judge Model. Adapt each component within  $StateEmb$  to the same dimension, then fuse them as a joint embedding to learn termination classification.

Our evaluation of the environment points out that occasionally more than one instance of object type  $c$  could be visible, Pal et al. (2021) deals with this by averaging their bounding box center and area by default, but if two instances with the identical object type of large size show in one frame, the averaged bounding box might cover a lot of irrelevant smaller objects with other types. Moreover, since our judge model will receive information from the context matrix as input, such an approach leads to the problem of providing dirty data. In contrast, when multiple instances of type  $c$  occur in the same frame, we take the one with the largest  $Bbx$  to represent the class. The learned node embedding and the flattened context matrix are concatenated as joint embedding, passed to an LSTM cell, and sent to the A3C model to learn the control action distribution  $P_{con}$ .

**Judge Model Branch.** At each time step  $t$ , if  $Done$  is sampled by the DRL branch, the judge model branch processes the flattened image feature  $ImgEmb_t$  of the observation, extracted via a pre-trained ResNet-18 (He et al., 2016) encoder. This encoder is pre-trained on ImageNet (Deng et al., 2009), encompassing 1000 object classes. By evaluating the context matrix obtained from the reinforcement learning branch, the judge model branch selects the target row with  $CS = 1.0$  as the target state vector. The image features  $ImgEmb_t$ , target state vector  $TagVec_t$  from the context matrix, and glove word embedding of the target  $GloveEmb_t$  are concatenated to form a state embedding  $StateEmb_t$ . The judge model is trained only on *Effective States* — states where the target is visible in the observation. If the target is not visible in the current frame (as indicated by  $b = 0$  in  $StateEmb_t$ ), the current time step is ignored by the judge model, yielding no output. If the target is visible,  $StateEmb_t$  is passed to the judge model. The output is then forwarded to the action control module. The agent acts on the final output action decided by the action control model and receives the reward signal. Analysis of the reward range reveals that successful episodes yield rewards in the range  $R_t \in [4.05, 4.90]$ . If  $R_t \geq 4.0$ , the ground truth for time step  $t$  is set as positive; otherwise, it’s set as negative. The ground truth of time step  $t$  and the  $StateEmb$  are stored as learning data in a "Batch Buffer" with a capacity of 64 samples. Upon reaching the maximum batch size, these samples serve as a training batch for the judge model to update the weights. This progress is illustrated in Figure 3.

Judge model is a supervised binary classification neural network with expanding and squeezing layers, as shown in Figure 4, these layers map the input *StateEmb* into the same dimension by several stacked linear layers, since *GloveEmb* might contain negative floating numbers, we observe that applying ReLU activation after linear layers causes the gradient of large partition of neurons to be zero, therefore we use Leaky ReLU (Xu et al., 2015) activation following the linear layers to prevent dead ReLU problem (Lu et al., 2019). Eventually, concatenate *ImgEmb*, *GloveEmb*, and *TecVec* together to form a joint embedding, and output the classification result with probabilities for whether to sample termination. In addition, because our data is collected online by reinforcement learning, during an episode, as mentioned in section 3.1, since the success condition requires the agent to terminate within a certain range of the target, most of the *Effective States* comes with ground truth of the negative class, where the agent should not terminate, this imbalance of training data causes long tail problem (Zhang et al., 2023). In our method, we use Focal Loss proposed by Lin et al. (2017) as our loss function as an alternative to Cross Entropy Loss:

$$FL(p_t) = -(1 - p_t)^\gamma \log(p_t) \quad (1)$$

Focal loss dynamically adjusts the weight of each instance in the loss function, focusing more on hard-to-classify instances and less on easy ones. We set  $\gamma = 0.7$  in our experiments.

$$a_t = \begin{cases} Done, & \text{if } p_d + p_\lambda \geq 1.5 \\ P_{con}, & \text{if } p_d \text{ is sampled} \\ P_{sub}, & \text{if } p_n \text{ is sampled} \end{cases} \quad (2)$$

**Action Control.** Action control directly samples the action from the output of reinforcement learning branch  $P_{con}$  in training. However, in the testing phase, the action model relies on probability distributions generated by two models  $P_{con}$  and  $P_{out}$ , and the action model outputs the final action  $a_t = Done$  if both models express sufficient confidence in terminating the episode.

Specifically, note the probability output of action *Done* from  $P_{con}$  as  $p_\lambda$ , and the probability of sample termination action in  $P_{out}$  as  $p_d$ , output  $a_t = Done$  when the sum of the confidence for termination action in two distributions satisfies  $p_d + p_\lambda \geq 1.5$ . Otherwise, according to the output of the judge model, while  $p_d$  is sampled from the output of the judge model, indicating that termination is advisable at the current time step, action control outputs final action  $a_t \in P_{con}$ . On the other hand, if  $p_n$  is sampled by the judge model, suggesting that termination should be delayed, action control outputs final action  $a_t \in P_{sub}$  with  $P_{sub}$  being a subset of  $P_{con}$  without *Done* action. This decision process is formally represented in Equation 2.

## 4. Experiment Results

**Environment & Dataset.** We use AI2-THOR (Kolve et al., 2017) as our environment simulator to evaluate our method for object navigation. AI2-THOR contains 120 different rooms with 30 rooms per room type Kitchen, Bedroom, Living room, and Bathroom. The rooms were split as training data and testing data, in our experiments, we use 80 rooms as training data, with 20 rooms from each room type. The remaining 40 rooms were used for testing. Amount all object categories in AI2-THOR environment  $|C_{total}| = 101$ .



	All		L $\geq$ 5	
	SR(%)	SPL(%)	SR(%)	SPL(%)
Random	10.4	3.2	0.6	0.4
Target-driven VN (Zhu et al., 2017)	35.0	10.3	25.0	10.5
Scene Prior (Yang et al., 2018)	35.4	10.9	23.8	10.7
SAVN (Wortsman et al., 2019)	35.7	9.3	23.9	9.4
MJOLNIR-r (Pal et al., 2021)	54.8	19.2	41.7	18.9
MJOLNIR-o (Pal et al., 2021)	65.3	21.1	50.0	20.9
<b>DITA (Ours)</b>	<b>71.4</b>	<b>21.6</b>	<b>57.9</b>	<b>22.2</b>

Table 1: Experiment results with comparisons to other methods in AI2-THOR.

**Evaluation Metrics.** The comparison of models was conducted using two metrics, in line with previous research (Zhu et al., 2017; Wortsman et al., 2019). *Success Rate (SR)* measures the probability of agent success in the environment, computed by  $SR = \frac{1}{N} \sum_{n=0}^N S_n$ ,  $N$  is the number of total episodes in evaluation, and  $S_n$  is a binary indicator with  $S_n = 1$  represents agent succeed in episode  $n$ . In addition, we use *Success Weighted by Path Length (SPL)*, which measures the navigation efficiency of the agent, defined as  $SPL = \frac{1}{N} \sum_{n=0}^N S_n \frac{O_n}{\max(L_n, O_n)}$  Where  $O_n$  is the length of the optimal path to the target that agent could take in episode  $n$ ,  $L_n$  is the actual path length agent has taken.

#### 4.1. Compared Methods

We compare our method with other end-to-end reinforcement learning-based methods: - **Random** In a random model, the agent navigates in the environment by randomly sampled action. - **Target-driven VN** (Zhu et al., 2017) Only fusions the observation of agent and the target embedding as input states to the model. - **Scene Prior** (Yang et al., 2018) This model incorporates semantic object relations as knowledge graph to the agent, learning from a joint embedding consisting of knowledge graph node embedding, image-wise observation features from pre-trained ResNet-18 and target word embedding. - **SAVN** (Wortsman et al., 2019) This model leverages meta-learning for the agent to learn the environment in both training and inferring. - **MJOLNIR-o** (Pal et al., 2021) This model integrates hierarchical object relationships to the agent by reward shaping, and learning object-wise observation features by constructing a context matrix from an object detector. - **MJOLNIR-r** (Pal et al., 2021) MJOLNIR-r is an alternative version of the MJOLNIR-o model, which passes image-wise observation features to the agent rather than object-wise observation.

#### 4.2. Results

By constructing *StateEmb* and passing it as input data, together with the reward signal, we have successfully trained a model to effectively recognize termination and handle termination action jointly with reinforcement learning, Figure 5 illustrates the convergence of training loss of the judge model.

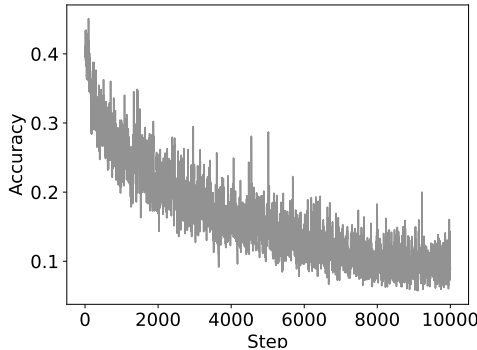


Figure 5: Training Loss of Judge Model with Smooth Factor  $\beta = 0.8$ .

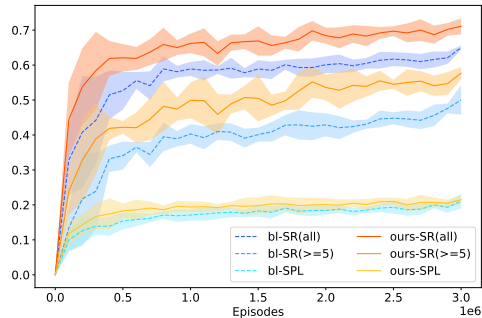


Figure 6: Test Accuracy of DITA and Baseline Model over 3 random seeds.

Compared with other map-less end-to-end models in Table 1 and Figure 6, it is evident that DITA demonstrates superior performance, particularly when compared to MJOLNIR-o. DITA exhibits a remarkable improvement of 9.3% across all room types. Furthermore, DITA showcases a remarkable 15.8% increase in episodes with optimal lengths ( $L \geq 5$ ). The significant improvements can be attributed to the novel architecture of DITA and its ability to implicitly infer object-wise depth information. This critical component helps to solve the problem of termination recognition in long episodes which other models struggle to handle effectively. By inferring depth information, DITA can better understand when the agent is close enough to the target object to end the episode successfully. This mechanism improves the success rate, especially in environments with long optimal episode lengths, Table 2 offers a detailed performance breakdown of DITA and other models by room types. In environments with large size (hence larger episode length) and complex layouts like living rooms, which make navigation more challenging our DITA significantly surpasses all the other models in both metrics, achieving a success rate of 75.6% and an SRL of 22.2%. Our results demonstrate the effectiveness of considering episode termination separately for the deep reinforcement learning model. It is noticeable that in the case of the Bathroom environment of our result, MJOLNIR-o achieves the highest success rate (SR). Indicates that DITA is capable of effectively navigating more confined and object-dense environments. We observed modest improvements in Success Weighted by Path Length (SRL). These results underscore the challenges involved in path planning and termination recognition in such scenarios.

## 5. Discussions

### 5.1. Limitations and Future Work

We have conducted failure cases analysis for DITA model, mainly the agent fails in the following cases: (1) Target object needs a precise path to navigate to. For example, a pillow of a double bed in a narrow room, where an agent needs to navigate precisely to the front corner of the bed, indicates the agent might still need an explicit planning component. (2) We observe that the training time required for training DITA is dominating all other

Model	Bath Room		Bedroom		Kitchen		Living Room		Avg.	
	SR(%)	SRL(%)	SR(%)	SRL(%)	SR(%)	SRL(%)	SR(%)	SRL(%)	SR(%)	SRL(%)
Target-driven VN (Zhu et al., 2017)	53.2	13.4	28.8	9.0	32.4	10.9	35.2	10.0	37.4	10.8
Scene Prior (Yang et al., 2018)	41.6	13.3	33.6	10.4	26.4	9.1	36.0	9.9	34.4	10.7
SAVN (Wortsman et al., 2019)	47.6	14.6	21.6	6.7	34.8	8.3	40.0	9.0	36.9	9.7
MJOLNIR-r (Pal et al., 2021)	72.8	24.3	41.2	16.9	56.4	21.2	50.8	15.9	55.3	19.6
MJOLNIR-o (Pal et al., 2021)	<b>82.4</b>	<b>25.1</b>	43.2	14.4	<b>74.8</b>	22.9	50.0	17.9	62.6	20.1
<b>DITA (Ours)</b>	63.2	20.1	<b>61.5</b>	<b>18.6</b>	73.0	<b>23.0</b>	<b>75.6</b>	<b>22.2</b>	<b>68.3</b>	<b>21.0</b>

Table 2: Experiment results by room types.

tested models, involving some efficient methods to the architecture might even boost the performance.

## 5.2. Conclusion

This paper presents the Depth-Inference Termination Agent (DITA), a novel approach designed to tackle the challenge of object navigation in autonomous navigation systems. Focusing specifically on the issues of target approach and episode termination in environments with lengthy optimal episode length, our approach has shown promising results in overcoming limitations faced by conventional Deep Reinforcement Learning (DRL) methods. Our experimental results, conducted within the AI2-THOR framework, clearly illustrate the superior performance of DITA. Our experiment results also highlight opportunities for further enhancements, possibly through the refinement of depth estimation, exploration strategies, or incorporation of additional environmental cues.

## References

- Marcin Andrychowicz, Filip Wolski, Alex Ray, Jonas Schneider, Rachel Fong, Peter Welinder, Bob McGrew, Josh Tobin, OpenAI Pieter Abbeel, and Wojciech Zaremba. Hindsight experience replay. *Advances in neural information processing systems*, 30, 2017.
- James Andrew Bagnell, David Bradley, David Silver, Boris Sofman, and Anthony Stentz. Learning for autonomous navigation. *IEEE Robotics & Automation Magazine*, 17(2): 74–84, 2010.
- Devendra Singh Chaplot, Dhiraj Gandhi, Saurabh Gupta, Abhinav Gupta, and Ruslan Salakhutdinov. Learning to explore using active neural slam. *arXiv preprint arXiv:2004.05155*, 2020a.
- Devendra Singh Chaplot, Dhiraj Prakashchand Gandhi, Abhinav Gupta, and Russ R Salakhutdinov. Object goal navigation using goal-oriented semantic exploration. *Advances in Neural Information Processing Systems*, 33:4247–4258, 2020b.
- Jia Deng, Wei Dong, Richard Socher, Li-Jia Li, Kai Li, and Li Fei-Fei. Imagenet: A large-scale hierarchical image database. In *2009 IEEE Conference on Computer Vision and Pattern Recognition*, pages 248–255, 2009. doi: 10.1109/CVPR.2009.5206848.

- Sam Michael Devlin and Daniel Kudenko. Dynamic potential-based reward shaping. In *Proceedings of the 11th international conference on autonomous agents and multiagent systems*, pages 433–440. IFAAMAS, 2012.
- An Dinh Vuong, Toan Tien Nguyen, Minh Nhat VU, Baoru Huang, Dzung Nguyen, Huynh Thi Thanh Binh, Thieu Vo, and Anh Nguyen. Habcrowd: A high performance simulator for crowd-aware visual navigation. *arXiv e-prints*, pages arXiv–2306, 2023.
- Raphael Druon, Yusuke Yoshiyasu, Asako Kanezaki, and Alassane Watt. Visual object search by learning spatial context. *IEEE Robotics and Automation Letters*, 5(2):1279–1286, 2020.
- Heming Du, Xin Yu, and Liang Zheng. Learning object relation graph and tentative policy for visual navigation. In *Computer Vision–ECCV 2020: 16th European Conference, Glasgow, UK, August 23–28, 2020, Proceedings, Part VII 16*, pages 19–34. Springer, 2020.
- Heming Du, Xin Yu, and Liang Zheng. Vtnet: Visual transformer network for object goal navigation. *arXiv preprint arXiv:2105.09447*, 2021.
- Jorge Fuentes-Pacheco, José Ruiz-Ascencio, and Juan Manuel Rendón-Mancha. Visual simultaneous localization and mapping: a survey. *Artificial intelligence review*, 43:55–81, 2015.
- Rui Fukushima, Kei Ota, Asako Kanezaki, Yoko Sasaki, and Yusuke Yoshiyasu. Object memory transformer for object goal navigation. In *2022 International Conference on Robotics and Automation (ICRA)*, pages 11288–11294, 2022. doi: 10.1109/ICRA46639.2022.9812027.
- Tuomas Haarnoja, Aurick Zhou, Pieter Abbeel, and Sergey Levine. Soft actor-critic: Off-policy maximum entropy deep reinforcement learning with a stochastic actor. In *International conference on machine learning*, pages 1861–1870. PMLR, 2018.
- Kaiming He, Xiangyu Zhang, Shaoqing Ren, and Jian Sun. Deep residual learning for image recognition. In *2016 IEEE Conference on Computer Vision and Pattern Recognition (CVPR)*, pages 770–778, 2016. doi: 10.1109/CVPR.2016.90.
- Jonathan Ho and Stefano Ermon. Generative adversarial imitation learning. *Advances in neural information processing systems*, 29, 2016.
- Yujing Hu, Weixun Wang, Hangtian Jia, Yixiang Wang, Yingfeng Chen, Jianye Hao, Feng Wu, and Changjie Fan. Learning to utilize shaping rewards: A new approach of reward shaping. *Advances in Neural Information Processing Systems*, 33:15931–15941, 2020.
- Tommi Jaakkola, Satinder Singh, and Michael Jordan. Reinforcement learning algorithm for partially observable markov decision problems. *Advances in neural information processing systems*, 7, 1994.

- Bilal Kartal, Pablo Hernandez-Leal, and Matthew E Taylor. Terminal prediction as an auxiliary task for deep reinforcement learning. In *Proceedings of the AAAI Conference on Artificial Intelligence and Interactive Digital Entertainment*, volume 15, pages 38–44, 2019.
- Apoorv Khandelwal, Luca Weihs, Roozbeh Mottaghi, and Aniruddha Kembhavi. Simple but effective: Clip embeddings for embodied ai. In *Proceedings of the IEEE/CVF Conference on Computer Vision and Pattern Recognition*, pages 14829–14838, 2022.
- Eric Kolve, Roozbeh Mottaghi, Winson Han, Eli VanderBilt, Luca Weihs, Alvaro Herrasti, Matt Deitke, Kiana Ehsani, Daniel Gordon, Yuke Zhu, et al. Ai2-thor: An interactive 3d environment for visual ai. *arXiv preprint arXiv:1712.05474*, 2017.
- Ranjay Krishna, Yuke Zhu, Oliver Groth, Justin Johnson, Kenji Hata, Joshua Kravitz, Stephanie Chen, Yannis Kalantidis, Li-Jia Li, David A Shamma, et al. Visual genome: Connecting language and vision using crowdsourced dense image annotations. *International journal of computer vision*, 123:32–73, 2017.
- Iro Laina, Christian Rupprecht, Vasileios Belagiannis, Federico Tombari, and Nassir Navab. Deeper depth prediction with fully convolutional residual networks. In *2016 Fourth international conference on 3D vision (3DV)*, pages 239–248. IEEE, 2016.
- Tsung-Yi Lin, Priya Goyal, Ross Girshick, Kaiming He, and Piotr Dollár. Focal loss for dense object detection. In *Proceedings of the IEEE international conference on computer vision*, pages 2980–2988, 2017.
- Lu Lu, Yeonjong Shin, Yanhui Su, and George Em Karniadakis. Dying relu and initialization: Theory and numerical examples. *arXiv preprint arXiv:1903.06733*, 2019.
- Stephanie Milani, Arthur Juliani, Ida Momennejad, Raluca Georgescu, Jaroslaw Rzepecki, Alison Shaw, Gavin Costello, Fei Fang, Sam Devlin, and Katja Hofmann. Navigates like me: Understanding how people evaluate human-like ai in video games. In *Proceedings of the 2023 CHI Conference on Human Factors in Computing Systems*, pages 1–18, 2023.
- Piotr Mirowski, Razvan Pascanu, Fabio Viola, Hubert Soyer, Andrew J Ballard, Andrea Banino, Misha Denil, Ross Goroshin, Laurent Sifre, Koray Kavukcuoglu, et al. Learning to navigate in complex environments. *arXiv preprint arXiv:1611.03673*, 2016.
- Volodymyr Mnih, Adria Puigdomenech Badia, Mehdi Mirza, Alex Graves, Timothy Lillicrap, Tim Harley, David Silver, and Koray Kavukcuoglu. Asynchronous methods for deep reinforcement learning. In *International conference on machine learning*, pages 1928–1937. PMLR, 2016.
- Giuseppe Oriolo, Marilena Vendittelli, and Giovanni Ulivi. On-line map building and navigation for autonomous mobile robots. In *Proceedings of 1995 IEEE international conference on robotics and automation*, volume 3, pages 2900–2906. IEEE, 1995.
- Georg Ostrovski, Marc G Bellemare, Aäron Oord, and Rémi Munos. Count-based exploration with neural density models. In *International conference on machine learning*, pages 2721–2730. PMLR, 2017.

- Anwesan Pal, Yiding Qiu, and Henrik Christensen. Learning hierarchical relationships for object-goal navigation. In *Conference on Robot Learning*, pages 517–528. PMLR, 2021.
- Deepak Pathak, Pulkit Agrawal, Alexei A Efros, and Trevor Darrell. Curiosity-driven exploration by self-supervised prediction. In *International conference on machine learning*, pages 2778–2787. PMLR, 2017.
- Jeffrey Pennington, Richard Socher, and Christopher Manning. GloVe: Global vectors for word representation. In *Proceedings of the 2014 Conference on Empirical Methods in Natural Language Processing (EMNLP)*, pages 1532–1543, Doha, Qatar, October 2014. Association for Computational Linguistics. doi: 10.3115/v1/D14-1162. URL <https://aclanthology.org/D14-1162>.
- Santhosh Kumar Ramakrishnan, Devendra Singh Chaplot, Ziad Al-Halah, Jitendra Malik, and Kristen Grauman. Poni: Potential functions for objectgoal navigation with interaction-free learning. In *Proceedings of the IEEE/CVF Conference on Computer Vision and Pattern Recognition*, pages 18890–18900, 2022.
- Ram Ramrakhya, Eric Undersander, Dhruv Batra, and Abhishek Das. Habitat-web: Learning embodied object-search strategies from human demonstrations at scale. In *Proceedings of the IEEE/CVF Conference on Computer Vision and Pattern Recognition*, pages 5173–5183, 2022.
- Anurag Ranjan, Varun Jampani, Lukas Balles, Kihwan Kim, Deqing Sun, Jonas Wulff, and Michael J Black. Competitive collaboration: Joint unsupervised learning of depth, camera motion, optical flow and motion segmentation. In *Proceedings of the IEEE/CVF conference on computer vision and pattern recognition*, pages 12240–12249, 2019.
- Jing Ren, Xishi Huang, and Raymond N. Huang. Efficient deep reinforcement learning for optimal path planning. *Electronics*, 11(21), 2022. ISSN 2079-9292. doi: 10.3390/electronics11213628. URL <https://www.mdpi.com/2079-9292/11/21/3628>.
- Manolis Savva, Angel X Chang, Alexey Dosovitskiy, Thomas Funkhouser, and Vladlen Koltun. Minos: Multimodal indoor simulator for navigation in complex environments. *arXiv preprint arXiv:1712.03931*, 2017.
- Petru Soviany, Radu Tudor Ionescu, Paolo Rota, and Nicu Sebe. Curriculum learning: A survey. *International Journal of Computer Vision*, 130(6):1526–1565, 2022.
- Bradly C Stadie, Sergey Levine, and Pieter Abbeel. Incentivizing exploration in reinforcement learning with deep predictive models. *arXiv preprint arXiv:1507.00814*, 2015.
- Fan Wang, Chaofan Zhang, Wen Zhang, Cuiyun Fang, Yingwei Xia, Yong Liu, and Hao Dong. Object-based reliable visual navigation for mobile robot. *Sensors*, 22(6), 2022. ISSN 1424-8220. doi: 10.3390/s22062387. URL <https://www.mdpi.com/1424-8220/22/6/2387>.
- Erik Wijmans, Manolis Savva, Irfan Essa, Stefan Lee, Ari S Morcos, and Dhruv Batra. Emergence of maps in the memories of blind navigation agents. *arXiv preprint arXiv:2301.13261*, 2023.

- Mitchell Wortsman, Kiana Ehsani, Mohammad Rastegari, Ali Farhadi, and Roozbeh Mottaghi. Learning to learn how to learn: Self-adaptive visual navigation using meta-learning. In *Proceedings of the IEEE/CVF conference on computer vision and pattern recognition*, pages 6750–6759, 2019.
- Bing Xu, Naiyan Wang, Tianqi Chen, and Mu Li. Empirical evaluation of rectified activations in convolutional network. *arXiv preprint arXiv:1505.00853*, 2015.
- Wei Yang, Xiaolong Wang, Ali Farhadi, Abhinav Gupta, and Roozbeh Mottaghi. Visual semantic navigation using scene priors. *arXiv preprint arXiv:1810.06543*, 2018.
- Joel Ye, Dhruv Batra, Abhishek Das, and Erik Wijmans. Auxiliary tasks and exploration enable objectnav. *arXiv preprint arXiv:2104.04112*, 2021.
- Sixian Zhang, Xinhang Song, Yubing Bai, Weijie Li, Yakui Chu, and Shuqiang Jiang. Hierarchical object-to-zone graph for object navigation. In *Proceedings of the IEEE/CVF international conference on computer vision*, pages 15130–15140, 2021.
- Yifan Zhang, Bingyi Kang, Bryan Hooi, Shuicheng Yan, and Jiashi Feng. Deep long-tailed learning: A survey. *IEEE Transactions on Pattern Analysis and Machine Intelligence*, 2023.
- Chuanxia Zheng, Tat-Jen Cham, and Jianfei Cai. T2net: Synthetic-to-realistic translation for solving single-image depth estimation tasks. In *Proceedings of the European conference on computer vision (ECCV)*, pages 767–783, 2018.
- Tinghui Zhou, Matthew Brown, Noah Snavely, and David G Lowe. Unsupervised learning of depth and ego-motion from video. In *Proceedings of the IEEE conference on computer vision and pattern recognition*, pages 1851–1858, 2017.
- Fengda Zhu, Xiwen Liang, Yi Zhu, Qizhi Yu, Xiaojun Chang, and Xiaodan Liang. Soon: Scenario oriented object navigation with graph-based exploration. In *Proceedings of the IEEE/CVF Conference on Computer Vision and Pattern Recognition*, pages 12689–12699, 2021.
- Yuke Zhu, Roozbeh Mottaghi, Eric Kolve, Joseph J Lim, Abhinav Gupta, Li Fei-Fei, and Ali Farhadi. Target-driven visual navigation in indoor scenes using deep reinforcement learning. In *2017 IEEE international conference on robotics and automation (ICRA)*, pages 3357–3364. IEEE, 2017.

## Appendix A. Reward Supervised Parallel Training

We train our reinforcement learning model and judge model in parallel, at time step  $t$ , the reinforcement learning model outputs control action distribution  $P_{con}$ , and the judge model outputs termination action distribution  $P_{out}$  given  $StateEmb_t$  from *Context Matrix*. Action control receives two outputs and decides the final action  $a_t$ , then in time step  $t+1$ , the reinforcement learning agent learns by the reward  $Reward_t$  returned from the environment, whereas judge model transfers  $Reward_t$  into ground truth supervision signal  $SupSign_t$  and

store it with  $StateEmb_t$  as a sample data in *Batch Buffer*, and updates itself once every 64 sample were collected. Figure 7 demonstrates this progress.

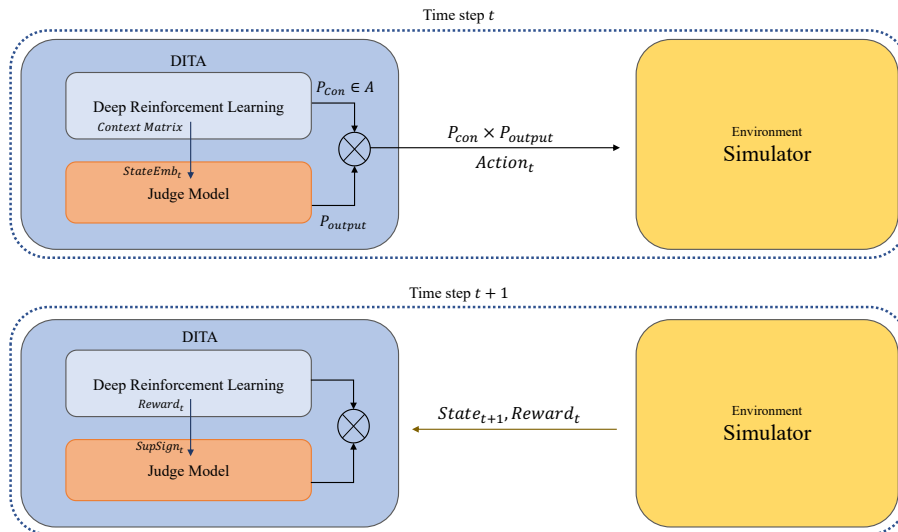


Figure 7: Reward Supervised Parallel Training.

## Appendix B. Target Object List

Room	Possible Target Object
Kitchen	Toaster, Spatula, Bread, Mug, CoffeeMachine, Apple
Living room	Painting, Laptop, Television, RemoteControl, Vase, ArmChair
Bedroom	Blinds, DeskLamp, Pillow, AlarmClock, CD
Bathroom	Mirror, ToiletPaper, SoapBar, Towel, SprayBottle

Table 3: List of Target Objects

## Appendix C. Implementation Details

We concurrently trained our judge model branch and the reinforcement learning branch with initially 1.6M episodes until we empirically observed that the judge model’s accuracy had saturated, we then froze the judge model branch and continued to train the reinforcement learning branch with in total of 3.0M episodes for all models. Our training/testing division is consistent with [Pal et al. \(2021\)](#); [Wortsman et al. \(2019\)](#). Models were trained on offline data collected from AI2-THOR v1.0.1. The A3C algorithm used in models was trained on 8 workers.